Optics Communications 316 (2014) 56–60

Contents lists available at ScienceDirect

Optics Communications

journal homepage: www.elsevier.com/locate/optcom

Influence of metal doping on optical properties of Si nanoparticles

A.B. Evlyukhin [a,*], A.L. Stepanov [b], A.V. Dmitriev [c], A.S. Akhmanov [d], V.N. Bagratashvili [d], B.N. Chichkov [a,d]

[a] Laser Zentrum Hannover e.V., Hollerithallee 8, D-30419 Hannover, Germany
[b] Kazan Physical-Technical Institute of RAS, Sibirsky Trakt 10/7, 420029 Kazan, Russia
[c] The Faculty of Physics, M.V. Lomonosov Moscow State University, Moscow 119991, Russia
[d] Institute of Laser and Information Technologies RAS, Moscow, Troitsk 142190, Russia

ARTICLE INFO

Article history:
Received 3 September 2013
Received in revised form
27 November 2013
Accepted 2 December 2013
Available online 12 December 2013

Keywords:
Silicon nanoparticles
Magnetic dipole
Electric dipole
Mie resonances

ABSTRACT

Spherical silicon nanoparticles with the sizes of 100–200 nm exhibit strong electric and magnetic dipole responses in the visible spectral range due to Mie resonances. At the resonance conditions, electromagnetic energy is accumulated inside Si nanoparticles, which can be used for the realization of efficient nanoantennas, nanolasers, and novel metamaterials. In this paper, modification of optical properties of Si nanoparticles by metal nanoinclusions, randomly distributed inside them, is theoretically investigated. The method is based on the recently developed, so-called, decomposed discrete dipole approximation (DDDA) allowing multipole analysis of light scattering by arbitrary shaped inhomogeneous nanoparticles. Particularly, the influence of metal nanoinclusions, their concentration and distribution, on the excitation of magnetic and electric dipole modes in Si nanoparticles is studied.

1. Introduction

Recently it has been shown first theoretically [1] and then experimentally [2,3] that crystalline silicon nanoparticles with the diameters of 100–200 nm exhibit strong electric and magnetic dipole responses in the visible spectral range. For larger submicron silicon particles, these resonances are shifted into the infrared region [4,5]. Explanation of these optical properties follows from Mie theory [6] demonstrating that the first and second lowest frequency resonances of dielectric spheres correspond to the excitation of magnetic and electric dipole modes [6,7]. At the resonant conditions, the incident electromagnetic energy is stored in the particle modes and the corresponding light scattering cross-section increases. These resonant optical properties of Si nanoparticles can be used for the creation of dielectric nanoantennas [8–11] and metamaterials with magnetic optical response [12,13]. Since Si nanoparticles are smaller than the light wavelengths, at the resonant conditions they can be considered as nanoscale electromagnetic energy concentrators. For example, for Si nanospheres with the diameter of 130 nm, the magnetic field corresponding to the magnetic dipole mode occupies the nanoparticle central region with the size of 40 nm [2]. Note that in contrast to metal nanoparticles, the electric and magnetic fields are concentrated inside the dielectric nanoparticles. Spectral positions of the resonances are determined by the particle sizes, their shape and internal solid structure. It has been demonstrated that by changing the aspect ratio of cylindrical Si nanoparticles it is possible to obtain the magnetic and electric dipole resonances at the same spectral wavelength [14,15]. It is known that the dielectric properties of the amorphous silicon differ from that of crystalline silicon. Therefore, optical resonances of the crystalline and amorphous Si nanoparticles having the same geometrical parameters are different [16].

In this paper, another possibility to change the resonant optical properties of crystalline Si nanoparticles by adding into their volume very small metal nanoinclusions (much smaller than the size of Si nanoparticles) is studied. Experimental realization of this approach can be performed using the metal ion implantation method [17].

2. Theoretical method

Our consideration is based on the method of decomposed discrete dipole approximation (DDDA) which combines the ordinary discrete dipole approximation (DDA) [18] with calculations of multipole moments of electric dipole systems [14]. Details of this method can be found elsewhere [14,19]. Briefly, in this approach the scattering object is replaced by a cubic lattice of electric point dipoles with a polarizability α_j. The corresponding dipole moment $\mathbf{p}_j$ induced in each lattice point j (with the radius-vector $\mathbf{r}_j$) is found by solving coupled-dipole equations. For the scattering particle located in a homogeneous surrounding, these equations

* Corresponding author. Tel.: +49 5112788236; fax: +49 5112788100.
E-mail address: a.evlyukhin@lzh.de (A.B. Evlyukhin).

0030-4018/$ - see front matter © 2013 Elsevier B.V. All rights reserved.
http://dx.doi.org/10.1016/j.optcom.2013.12.010

can be presented by [20]

$$\mathbf{p}_j = \alpha_j \mathbf{E}_0(\mathbf{r}_j) + \frac{k_0^2}{\varepsilon_0}\alpha_j \sum_{l\neq j}^{N} \hat{G}(\mathbf{r}_j, \mathbf{r}_l)\mathbf{p}_l, \tag{1}$$

where $\mathbf{E}_0(\mathbf{r})$ is the electric field of the incident (external) monochromatic electromagnetic wave with the angular frequency ω, $\hat{G}(\mathbf{r}_j, \mathbf{r}_l)$ is the Green tensor of this system without the scatterer [20], and N is the total number of point dipoles. Here k_0 is the wavenumber in vacuum, ε_0 is the vacuum dielectric constant. Detailed discussion of DDA realizations and their relation with Green's tensor approach can be found elsewhere [21].

After solution of Eqs. (1), the discrete dipole presentation of the electric dipole moment $\mathbf{p}$, electric quadrupole moment $\hat{Q}(\mathbf{r}_0)$, magnetic dipole moment $\mathbf{m}(\mathbf{r}_0)$, magnetic quadrupole moment $\hat{M}(\mathbf{r}_0)$, and electric octupole moment $\hat{O}(\mathbf{r}_0)$ of the scatterer with respect to the point $\mathbf{r}_0$ is presented by [14]

$$\mathbf{p} = \sum_{j=1}^{N} \mathbf{p}_j; \quad \hat{Q}(\mathbf{r}_0) = \sum_{j=1}^{N} \hat{Q}^j(\mathbf{r}_0); \quad \mathbf{m}(\mathbf{r}_0) = \sum_{j=1}^{N} \mathbf{m}_j(\mathbf{r}_0);$$
$$\hat{M}(\mathbf{r}_0) = \sum_{j=1}^{N} \hat{M}^j(\mathbf{r}_0); \quad \hat{O}(\mathbf{r}_0) = \sum_{j=1}^{N} \hat{O}^j(\mathbf{r}_0), \tag{2}$$

where the corresponding point multipole moments associated with the single electric dipole $\mathbf{p}_j$ are determined by

$$\hat{Q}^j(\mathbf{r}_0) = 3((\mathbf{r}_j - \mathbf{r}_0)\mathbf{p}_j + \mathbf{p}_j(\mathbf{r}_j - \mathbf{r}_0)), \tag{3}$$

$$\mathbf{m}_j(\mathbf{r}_0) = -\frac{i\omega}{2}[(\mathbf{r}_j - \mathbf{r}_0) \times \mathbf{p}_j], \tag{4}$$

$$\hat{M}^j(\mathbf{r}_0) = -\frac{i2\omega}{3}[(\mathbf{r}_j - \mathbf{r}_0) \times \mathbf{p}_j](\mathbf{r}_j - \mathbf{r}_0), \tag{5}$$

$$O^j_{\beta\beta\beta} = 3p_{j\beta}(\beta_j - \beta_0)^2, O^j_{\beta\beta\gamma} = O^j_{\beta\gamma\beta} = O^j_{\gamma\beta\beta} = 2p_{j\beta}(\beta_j - \beta_0)(\gamma_j - \gamma_0),$$
$$O^j_{\beta\gamma\tau} = p_{j\beta}(\gamma_j - \gamma_0)(\tau_j - \tau_0) + p_{j\gamma}(\beta_j - \beta_0)(\tau_j - \tau_0) + p_{j\tau}(\gamma_j - \gamma_0)(\beta_j - \beta_0), \tag{6}$$

where $\beta = x, y, z$, and $\gamma = x, y, z$, and $\tau = x, y, z$; moreover, $\beta \neq \gamma$, $\beta \neq \tau$, and $\tau \neq \gamma$; the electric dipole moment $\mathbf{p}_j$ has the coordinates (p_{jx}, p_{jy}, p_{jz}).

Finally, the scattered electric field in the far wave zone is presented by

$$\mathbf{E}(\mathbf{r}) \approx \frac{k_0^2 e^{ik_d(r - \mathbf{n}\cdot\mathbf{r}_0)}}{4\pi\varepsilon_0 r}\left([\mathbf{n} \times [\mathbf{p} \times \mathbf{n}]] + \frac{1}{v_d}[\mathbf{m}(\mathbf{r}_0) \times \mathbf{n}]\right.$$
$$+ \frac{ik_d}{6}[\mathbf{n} \times [\mathbf{n} \times \hat{Q}(\mathbf{r}_0)\mathbf{n}]] + \frac{ik_d}{2v_d}[\mathbf{n} \times (\hat{M}(\mathbf{r}_0)\mathbf{n})]$$
$$\left. + \frac{k_d^2}{6}[\mathbf{n} \times [\mathbf{n} \times \hat{O}(\mathbf{r}_0)(\mathbf{nn})]]\right), \tag{7}$$

where k_d and v_d are the wavenumber and the light phase velocity in the medium surrounding the scatterer, respectively. $\mathbf{n}$ is the unit vector directed along the $\mathbf{r}$.

Multipole decomposed extinction cross section σ_{ext} including first multipole terms is written as [14,19]

$$\sigma_{ext} \approx \frac{\omega}{2P_{in}} \mathrm{Im}\left(\mathbf{E}_0^*(\mathbf{r}_0) \cdot \mathbf{p} + \mu_0 \mathbf{H}_0^*(\mathbf{r}_0) \cdot \mathbf{m}(\mathbf{r}_0) + \frac{\mu_0[\nabla \mathbf{H}_0^*(\mathbf{r}_0)]^T : \hat{M}(\mathbf{r}_0)}{2}\right.$$
$$\left. + \frac{\{\nabla \mathbf{E}_0^*(\mathbf{r}_0) + (\nabla \mathbf{E}_0^*(\mathbf{r}_0))^T\} : \hat{Q}(\mathbf{r}_0)}{12} + \frac{1}{6}\sum_{\beta\gamma\tau} O_{\beta\gamma\tau}(\mathbf{r}_0)\frac{\partial^2}{\partial\gamma\partial\tau}E^*_{0\beta}(\mathbf{r}_0)\right), \tag{8}$$

where P_{in} is the radiation flux of the incident wave, μ_0 is the vacuum permeability, $\mathbf{H}_0(\mathbf{r}_0)$ is the magnetic field of the incident wave at the point $\mathbf{r}_0$. The values $\nabla\mathbf{E}_0(\mathbf{r}_0)$ and $\nabla\mathbf{H}_0(\mathbf{r}_0)$ are the tensorial gradients of the electric and magnetic fields, respectively, at the point $\mathbf{r}_0$ [14]. For homogeneous scatterers, the polarizabilities α_j in (1) are the same for every dipole in this system. However, if the scatterer contains some inhomogeneous regions, α_j will be dependent on the dipole position in the scatterer. In the quasi-static approximation with the "radiative reaction" correction [18], one can write

$$\alpha_j = \frac{\alpha_{0j}}{1 - ik_d^3\alpha_{0j}/(6\pi\varepsilon_d\varepsilon_0)}, \tag{9}$$

where

$$\alpha_{0j} = 3\varepsilon_d\varepsilon_0 V_j \frac{\varepsilon_j - \varepsilon_d}{\varepsilon_j + 2\varepsilon_d}, \tag{10}$$

V_j is the volume of the discretization cell with the number j, ε_j is its dielectric permittivity, ε_d is the dielectric permittivity of the surrounding medium (the medium outside the scatterer).

The total electric field $\mathbf{E}(\mathbf{r})$ outside the scatterer is the superposition of the incident $\mathbf{E}_0(\mathbf{r})$ and scattered $\mathbf{E}_{sc}(\mathbf{r})$ electric fields

$$\mathbf{E}_0(\mathbf{r}) = \mathbf{E}_0(\mathbf{r}) + \mathbf{E}_{sc}(\mathbf{r}) = \mathbf{E}_0(\mathbf{r}) + \frac{k_0^2}{\varepsilon_0}\sum_{l=1}^{N} \hat{G}(\mathbf{r}, \mathbf{r}_l)\mathbf{p}_l. \tag{11}$$

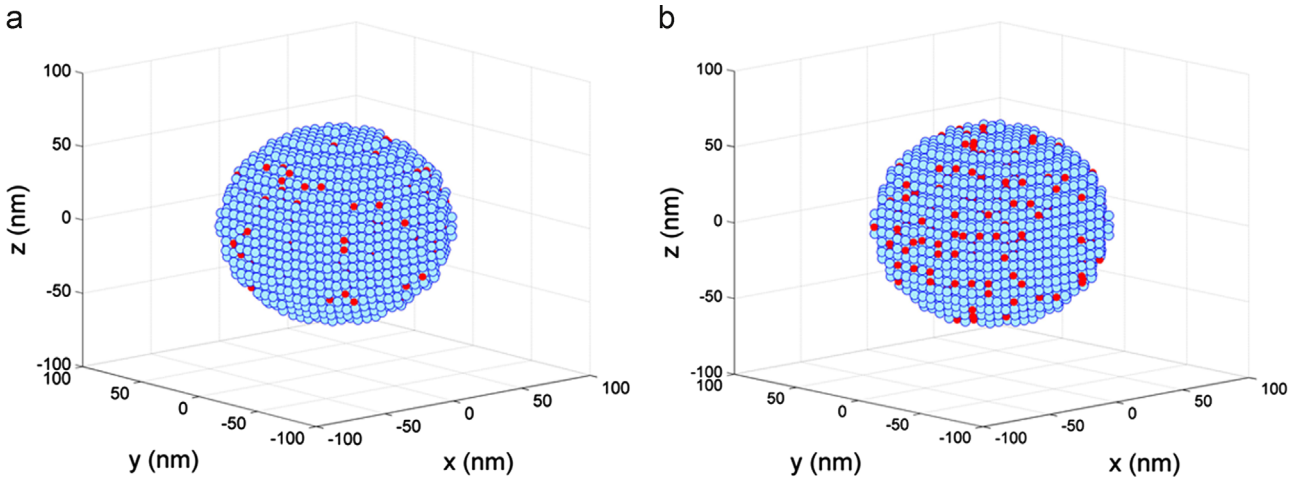

Fig. 1. Discrete dipole representation of spherical Si nanoparticles with the radius of 65 nm doped by Ag nanoparticles (red dots). Ag concentration (a) 5%, (b) 10%. (For interpretation of the references to color in this figure caption, the reader is referred to the web version of this paper.)